Appl. Comput. Harmon. Anal. • • • (• • • •) • • •–• • •

Contents lists available at ScienceDirect

Applied and Computational Harmonic Analysis

www.elsevier.com/locate/acha

A multifractal formalism for non-concave and non-increasing spectra: The leaders profile method

Céline Esser, Thomas Kleyntssens, Samuel Nicolay *

Université de Liège, Institut de Mathématique, Allée de la Découverte, 12, Bâtiment B37, B-4000 Liège (Sart-Tilman), Belgium

ARTICLE INFO

Article history:
Received 18 February 2015
Received in revised form 19 October 2015
Accepted 30 December 2015
Available online xxxx
Communicated by Stephane G. Mallat

MSC:
42C40
46E35
90C48
26A16

Keywords:
Multifractal formalism for functions
Wavelet leaders
L^ν spaces
Large deviation methods

ABSTRACT

We present an implementation of a multifractal formalism based on the types of histogram of wavelet leaders. This method yields non-concave spectra and is not limited to their increasing part. We show both from the theoretical and from the applied points of view that this approach is more efficient than the wavelet-based multifractal formalisms previously introduced.

1. Introduction

Multifractal analysis initially appeared in the context of fully developed turbulence [1]; the aim was to study the Hölder regularity of a signal. Let us be more precise about this notion. A locally bounded function $f : \mathbf{R}^n \to \mathbf{R}$ belongs to the Hölder space $\Lambda^\alpha(x_0)$ (with $x_0 \in \mathbf{R}^n$ and $\alpha \geq 0$) if there exist a constant $C > 0$ and a polynomial P_{x_0} of degree less than α such that

$$|f(x) - P_{x_0}(x)| < C|x - x_0|^\alpha \tag{1}$$

* Corresponding author. Fax: +32 43669547.
E-mail address: S.Nicolay@ulg.ac.be (S. Nicolay).

http://dx.doi.org/10.1016/j.acha.2015.12.006
1063-5203/

in a neighborhood of x_0. The polynomial is clearly unique and one has $\Lambda^{\alpha+\varepsilon}(x_0) \subset \Lambda^{\alpha}(x_0)$ for any $\varepsilon \geq 0$. The Hölder exponent of f at x_0 is defined by

$$h_f(x_0) = \sup\{\alpha \geq 0 : f \in \Lambda^{\alpha}(x_0)\}.$$

As usual, a function f belongs to $\Lambda^{\alpha}(\mathbf{R}^n)$ if f belongs to $\Lambda^{\alpha}(x_0)$ for any x_0, the constant C in (1) being uniform.

If the signal f is highly irregular, determining $h_f(x_0)$ for each x_0 is meaningless, since the function h_f can be itself very irregular. One tries instead to estimate the "size" of the iso-Hölder sets E_h, that is the sets of points sharing the same Hölder exponent h:

$$E_h = \{x \in \mathbf{R}^n : h_f(x) = h\}.$$

Such sets can be fractal sets, therefore by "size" one usually means Hausdorff dimension $\dim_{\mathcal{H}}$ (see e.g. [2]). The Hölder spectrum of f defined as

$$d_f : [0, +\infty] \to \{-\infty\} \cup [0, n] \quad h \mapsto \dim_{\mathcal{H}} E_h,$$

gives global information about the pointwise regularity of f.

Computing the Hölder spectrum by directly using the definition given above truly is an unattainable goal in most of the practical cases, but there exist heuristic methods to estimate d_f that give satisfactory results in many situations. Such a procedure is called a multifractal formalism; if it leads to the exact spectrum of the function f, one says that the multifractal formalism is satisfied for f. A method was first proposed by Parisi and Frisch [1]; later, Arneodo et al. proposed a similar method based on the continuous wavelet transform [3]. In both approaches, one tries to compute the function

$$\eta(q) = \sup\{s : f \in B^{s/q}_{q,\infty}\} \tag{2}$$

relying on the Besov spaces $B^s_{q,p}$ using the box-counting technique or wavelets [4], since heuristic arguments underlie the following equality:

$$d_f(h) = \inf_q \{hq - \eta(q)\} + n.$$

From a mathematical point of view, these methods only lead to an upper bound [4]. More precisely, if $f : \mathbf{R}^n \to \mathbf{R}$ is a locally bounded function belonging to $\Lambda^{\varepsilon}(\mathbf{R}^n)$ for some $\varepsilon > 0$, then

$$d_f(h) \leq \inf_{q > q_0} \{hq - \eta(q)\} + n,$$

where q_0 satisfies $\eta(q_0) = n$.

Since the Besov spaces $B^s_{q,p}$ are not defined for negative values of q, the decreasing part of the spectrum cannot be obtained using the method described above. To take care of this problem, Arneodo et al. proposed the wavelet transform modulus maxima (WTMM) method [5], using the notion of line of maxima in the wavelet transform. This technique proved helpful in many practical problems, but its theoretical contribution was limited; in particular, there is no underlying functional space. This is why Jaffard replaced the continuous wavelet transform with the discrete one and introduced the wavelet leaders method (WLM) [6], based on the oscillation spaces O^s_q [7]. These spaces are well defined for negative values of q and $s > n/q$ implies $O^s_q = B^s_{q,\infty}$. The idea consists in replacing Besov spaces in (2) with oscillation spaces to get

$$\eta(q) = \sup\{s : f \in O^{s/q}_q\}.$$

Please cite this article in press as: C. Esser et al., A multifractal formalism for non-concave and non-increasing spectra: The leaders profile method, Appl. Comput. Harmon. Anal. (2016), http://dx.doi.org/10.1016/j.acha.2015.12.006

When comparing the WTMM with the WLM, numerical results are similar [8], but there exists an upper bound associated to the WLM if f belongs to $\Lambda^{\varepsilon}(\mathbf{R}^n)$ for some $\varepsilon > 0$ [6]: in this case, one has

$$d_f(h) \leq \inf_q \{hq - \eta(q)\} + n.$$

Even with the WLM, a problem is still subsisting: in the multifractal formalisms presented above, the spectrum is obtained with an inverse Legendre transform and so is necessarily concave. However, it is possible to compute functions whose spectrum is not concave (see e.g. [9]). To overcome this second problem, Jaffard introduced a multifractal formalism which is heuristically based on the types of histogram of (discrete) wavelet coefficients [10]; for this reason, it will be called the wavelet profile method (WPM). If this formalism allows to effectively recover non-concave spectra, the problem met with the first approaches reappears: one cannot access the decreasing part of the spectrum through the WPM. The leaders profile method (LPM) [11] was created in order to combine the advantages of both the WLM and the WPM. The idea is to replace the wavelet coefficients in the WPM with the wavelet leaders. By doing so, one defines a new multifractal formalism that should lead to the detection of non-increasing and non-concave spectra.

In this paper, we present an implementation of the formalism based on the LPM. From a theoretical point of view, we prove that this method gives a sharper upper bound than the previous approaches and show its effectiveness by applying it to several examples. The remainder of this paper is structured as follows. We first introduce the three formalisms based on the discrete wavelet transform and describe an efficient way to implement the LPM. Next, we show that this approach is more theoretically sounds than the other ones considered here. We then switch to the practical point of view and show that, although the new technique is very efficient, it is complementary to the WLM.

2. Some multifractal formalisms

We briefly give here the three wavelet-based methods for estimating a Hölder spectrum we are going to work with. The first one is the well-known wavelet leaders method (WLM) [6], which can be seen as the discrete counterpart of the wavelet transform modulus maxima method [5,8]. Next, we recall the wavelet profile method (WPM) [10]; this method has recently been implemented [9]. Finally, we introduce the leaders profile method (LPM) [11], which can be seen as a combination of the two previous methods. Those three methods lead to an upper bound for the Hölder spectrum of any function f provided that f belongs to $\Lambda^{\varepsilon}(\mathbf{R}^n)$ for some $\varepsilon > 0$ [6,10,11]. Let us mention that both the WPM and the LPM can be assimilated to large deviation methods (see e.g. [12]).

2.1. The discrete wavelet transform

Let us briefly recall some definitions and notations (for more precisions, see e.g. [13–15]). Under some general assumptions, there exist a function ϕ and $2^n - 1$ functions $(\psi^{(i)})_{1 \leq i < 2^n}$, called wavelets, such that

$$\{\phi(x-k) : k \in \mathbf{Z}^n\} \cup \{\psi^{(i)}(2^j x - k) : 1 \leq i < 2^n, k \in \mathbf{Z}^n, j \in \mathbf{N}\}$$

form an orthogonal basis of $L^2(\mathbf{R}^n)$. Any function $f \in L^2(\mathbf{R}^n)$ can be decomposed as follows,

$$f(x) = \sum_{k \in \mathbf{Z}^n} C_k \phi(x-k) + \sum_{j \in \mathbf{N}} \sum_{k \in \mathbf{Z}^n} \sum_{1 \leq i < 2^n} c_{j,k}^{(i)} \psi^{(i)}(2^j x - k),$$

where

$$c_{j,k}^{(i)} = 2^{nj} \int_{\mathbf{R}^n} f(x) \psi^{(i)}(2^j x - k)\, dx$$

Please cite this article in press as: C. Esser et al., A multifractal formalism for non-concave and non-increasing spectra: The leaders profile method, Appl. Comput. Harmon. Anal. (2016), http://dx.doi.org/10.1016/j.acha.2015.12.006

and

$$C_k = \int_{\mathbf{R}^n} f(x)\phi(x-k)\,dx.$$

Let us remark that we do not choose the $L^2(\mathbf{R}^n)$ normalization for the wavelets, but rather an $L^\infty(\mathbf{R}^n)$ normalization, which is better fitted to the study of the Hölderian regularity.

On the torus $\mathbf{R}^n/\mathbf{Z}^n$, we will use the periodized wavelets

$$\psi_p^{(i)}(2^j x - k) = \sum_{l\in\mathbf{Z}^n} \psi^{(i)}(2^j(x-l)-k) \quad (j\in\mathbf{N},\ k\in\{0,\dots,2^j-1\}^n)$$

to form a basis of the one-periodic functions on $\mathbf{R}^n$ which locally belong to $L^2(\mathbf{R}^n)$ [16]. The corresponding coefficients $c_{j,k}^{(i)}$ are naturally called the periodized wavelet coefficients.

From now on, we shall systematically use the periodized wavelet coefficients and often omit any reference to the index i. For instance, the set $\{c_{j,k} : (j,k)\in E\}$ has to be understood as the set $\{c_{j,k}^{(i)} : (j,k)\in E,\ 1\le i<2^n\}$.

2.2. The wavelet leaders method

The WLM [6] is somehow an adaptation of the box-counting method [1] in the context of the discrete wavelet transform [8]. It is usually given for functions of $L^2(\mathbf{R}^n)$, but in practice, real-life data have compact support, so that we can work with periodic functions.

Let $\lambda_{j,k}^{(i)}$ denote the dyadic cube

$$\lambda_{j,k}^{(i)} = \frac{i}{2^{j+1}} + \frac{k}{2^j} + [0,\frac{1}{2^{j+1}})^n.$$

In the sequel, we will omit any reference to the indices i, j and k for such cubes by writing $\lambda = \lambda_{j,k}^{(i)}$. We will also index the wavelet coefficients of a function f with the dyadic cubes λ so that c_λ will refer to the quantity $c_{j,k}^{(i)}$. The set Λ_j will denote the set of dyadic cubes λ of $[0,1]^n$ with side 2^{-j}.

The wavelet leader associated to the cube λ is the quantity

$$d_\lambda = \sup_{\lambda'\subset 3\lambda} |c_{\lambda'}|.$$

By mimicking the box counting method, one sets

$$S_f(j,q) = 2^{-nj}\sum_{\lambda\in\Lambda_j} d_\lambda^q,$$

where the sum is restricted to the cubes λ such that $d_\lambda\neq 0$. From this, one sets

$$\eta_f(q) = \liminf_{j\to+\infty} \frac{\log S_f(j,q)}{\log 2^{-j}} \tag{3}$$

to define the multifractal formalism associated to the wavelet leaders as follows,

$$d_f^\eta(h) = \inf_q\{hq-\eta_f(q)\}+n. \tag{4}$$

The heuristic argument that underpins this method is a large deviation-type argument. Let us consider the quantity $\sum_\lambda d_\lambda^q$. One can show that if λ is a dyadic cube containing a point whose Hölder exponent is

Please cite this article in press as: C. Esser et al., A multifractal formalism for non-concave and non-increasing spectra: The leaders profile method, Appl. Comput. Harmon. Anal. (2016), http://dx.doi.org/10.1016/j.acha.2015.12.006

h, one has $d_\lambda \sim 2^{-hj}$ as j tends to infinity [6]. Since the number of such dyadic cubes λ should be about $2^{d_f(h)j}$, the total contribution should correspond to $2^{(d_f(h)-hq)j}$. Moreover, from the previous definitions, one can expect to have $\sum_\lambda d_\lambda^q \sim 2^{(-\eta_f(q)+n)j}$. The dominating contribution is the one corresponding to a value of h associated with the biggest exponent in $2^{(d_f(h)-hq)j}$, so that we are led to the following heuristic formula: $-\eta_f(q)+n = \sup_h\{d_f(h)-hq\}$. It can be shown that one has $d_f \leq d_f^\eta$ [6].

Let us make two remarks. First, spectrum (4) is necessarily concave. Secondly, the wavelet leaders give rise to some generalization of the Besov spaces called the oscillation spaces, which define a rigorous framework for studying multifractal functions [7].

2.3. The wavelet profile method

For the wavelet profile method, the idea is to look at the distribution of wavelet coefficients and try to obtain some kind of robust information [10], i.e. information that relies on the function and not on the chosen wavelet. It is therefore natural to consider

$$\rho_f(h) = \lim_{\varepsilon\to 0^+} \limsup_{j\to+\infty} \frac{\log \#\{\lambda \in \Lambda_j : 2^{-(h+\varepsilon)j} \leq |c_\lambda| < 2^{-(h-\varepsilon)j}\}}{\log 2^j},$$

where c_λ are the periodized wavelet coefficients of f and to apply an argument similar to the one given for the WLM. Considering dyadic cubes related to some Hölder exponent h, one has $d_\lambda \sim 2^{-hj}$ as previously stated. The number of such cubes should be about $2^{j\rho_f(h)}$ by definition. One therefore gets $\rho_f(h) = d_f(h)$, at least intuitively speaking. However, this density ρ_f is not well defined, since it depends on the chosen wavelet basis [10]. Moreover, it seems that no general relation can be obtained between ρ_f and d_f from a theoretical point of view [10]. To circumvent this problem, one can slightly modify this approach to obtain an efficient method.

One defines the wavelet profile of f by

$$\nu_f(h) = \lim_{\varepsilon\to 0^+} \limsup_{j\to+\infty} \frac{\log \#\{\lambda \in \Lambda_j : |c_\lambda| \geq 2^{-(h+\varepsilon)j}\}}{\log 2^j}.$$

One can show that the function ν_f is independent of the chosen wavelet basis [17]. It is obviously non-decreasing, right-continuous and there exists $h_{\min} \in \mathbf{R}$ for which $\nu_f(h) = -\infty$ for all $h < h_{\min}$ and $\nu_f(h) \in [0, n]$ for all $h \geq h_{\min}$. Moreover, $h_{\min} > 0$ if f belongs to $\Lambda^\varepsilon(\mathbf{R}^n)$ for some $\varepsilon > 0$. The wavelet profile gives, in some way, the asymptotic behavior of the number of coefficients that have a given order of magnitude: there are approximately $2^{\nu_f(h)j}$ wavelet coefficients whose modulus is greater than 2^{-hj}.

If $h_{\min} > 0$, the multifractal formalism based on the wavelet profile is defined as follows,

$$d_f^\nu(h) = \begin{cases} -\infty & \text{if } h < h_{\min} \\ \min\{h \sup\limits_{h'\in(0,h]} \dfrac{\nu_f(h')}{h'}, n\} & \text{if } h \geq h_{\min} \end{cases}.$$

Again, we have the following relation in the general case: $d_f \leq d_f^\nu$ [10].

The passage from ν_f to d_f^ν transforms the wavelet profile into a function with a special property, called the increasing-visibility [18]:

Definition 1. Take $0 \leq a < b \leq +\infty$. A function $g : [a, b] \mapsto [0, +\infty)$ is with *increasing-visibility* if g is continuous at a and

$$\sup_{y\in(a,x]} \frac{g(y)}{y} \leq \frac{g(x)}{x},$$

for all $x \in (a, b]$.

Please cite this article in press as: C. Esser et al., A multifractal formalism for non-concave and non-increasing spectra: The leaders profile method, Appl. Comput. Harmon. Anal. (2016), http://dx.doi.org/10.1016/j.acha.2015.12.006

In other words, a function g is with increasing-visibility if for all $x \in (a, b]$, the segment $[(0, 0), (x, g(x))]$ lies above the graph of g on $(a, x]$.

Of course, the WPM can only recover spectra with increasing-visibility. Moreover, since one considers wavelet coefficients and not wavelet leaders, this method can only lead to the increasing part of the spectrum [10]. The wavelet profile also gives rise to some generalization of the Besov spaces called S^ν spaces [19].

2.4. The leaders profile method

The leaders profile method aims at combining the advantages of the two previous methods [11]. With the use of the wavelet leaders, one can consider entire spectra, while the profile function allows to recover non-concave spectra.

With the same large deviation-type argument as in the previous section, one could be led to consider the following profile,

$$\tilde{\rho}_f(h) = \lim_{\varepsilon \to 0^+} \limsup_{j \to +\infty} \frac{\log \#\{\lambda \in \Lambda_j : 2^{-(h+\varepsilon)j} \leq d_\lambda < 2^{-(h-\varepsilon)j}\}}{\log 2^j},$$

so that there exist approximately $2^{\tilde{\rho}_f(h)j}$ wavelet leaders of amplitude 2^{-hj}. However, here again, $\tilde{\rho}_f$ depends on the chosen wavelet basis [11].

The idea is to modify the above definition as follows. Let h_s be the smallest positive real number such that $\tilde{\rho}_f(h_s) = n$. One sets

$$\tilde{d}_f(h) = \begin{cases} \lim_{\varepsilon \to 0^+} \limsup_{j \to +\infty} \frac{\log \#\{\lambda \in \Lambda_j : d_\lambda \geq 2^{-(h+\varepsilon)j}\}}{\log 2^j} & \text{if } h \leq h_s \\ \lim_{\varepsilon \to 0^+} \limsup_{j \to +\infty} \frac{\log \#\{\lambda \in \Lambda_j : d_\lambda \leq 2^{-(h-\varepsilon)j}\}}{\log 2^j} & \text{if } h \geq h_s \end{cases}. \tag{5}$$

It can be shown that the leaders profile $\tilde{d}_f$ does not depend on the chosen wavelet basis and that if $\tilde{\rho}_f$ takes the value $-\infty$ outside of a compact set of $(0, +\infty)$, $\tilde{d}_f$ is the increasing hull of $\tilde{\rho}_f$ on $(-\infty, h_s]$ and its decreasing hull on $[h_s, +\infty)$ [11]. Moreover, from the definition of $h_{\min}$, it is direct to see that $h_{\min} = \inf\{h : \tilde{d}_f(h) \geq 0\}$. As for the two other methods, we have $d_f \leq \tilde{d}_f$.

Finally, let us mention that the leaders profile gives rise to some generalization of the oscillation spaces called L^ν spaces [11].

2.5. An implementation of the leaders profile method

The implementation of the LPM is similar to that of the WPM [9]. Let us recall here the main ideas. It is based on the following proposition:

Proposition 1. *Let $\boldsymbol{C} = (C_j)_{j \in \mathbf{N}}$ be a sequence of positive numbers such that there exists $c > 0$ with $1/c \leq C_j \leq c$ for all $j \in \mathbf{N}$. If we denote*

$$\tilde{d}_f^{\boldsymbol{C}}(h) = \begin{cases} \lim_{\varepsilon \to 0^+} \limsup_{j \to +\infty} \frac{\log \#\{\lambda \in \Lambda_j : d_\lambda \geq C_j 2^{-(h+\varepsilon)j}\}}{\log 2^j} & \text{if } h \leq h_s \\ \lim_{\varepsilon \to 0^+} \limsup_{j \to +\infty} \frac{\log \#\{\lambda \in \Lambda_j : d_\lambda \leq C_j 2^{-(h-\varepsilon)j}\}}{\log 2^j} & \text{if } h \geq h_s \end{cases},$$

then $\tilde{d}_f^{\boldsymbol{C}}(h) = \tilde{d}_f(h)$ for all $h \in \mathbf{R}$.

Please cite this article in press as: C. Esser et al., A multifractal formalism for non-concave and non-increasing spectra: The leaders profile method, Appl. Comput. Harmon. Anal. (2016), http://dx.doi.org/10.1016/j.acha.2015.12.006

This result is a simple adaptation of the proof of Proposition 2 in [9] where the wavelet coefficients are replaced by the wavelet leaders. If $\boldsymbol{C}$ is the constant sequence $C_j = C$, we naturally denote $\tilde{d}_f^{\boldsymbol{C}}$ by $\tilde{d}_f^C$.

Notations. The sets $\{\lambda \in \Lambda_j : d_\lambda \geq C2^{-hj}\}$ (resp. $\{\lambda \in \Lambda_j : d_\lambda \leq C2^{-hj}\}$) will be denoted by $E^{\geq}(C,h)$ (resp. $E^{\leq}(C,h)$), and we set $h_{\max} = \sup\{h : \tilde{d}_f(h) \geq 0\}$.

The definition of $\tilde{d}_f^C(h)$ formalizes the idea that, if $h \in [h_{\min}, h_s]$ (resp. $h \in [h_s, h_{\max}]$), there are about $2^{\tilde{d}_f^C(h)j}$ wavelet leaders larger (resp. smaller) than $C2^{-hj}$ for j "large enough". So, it is natural to approximate $\tilde{d}_f^C(h)$ by the slope of

$$j \mapsto \frac{\log \# E_j^{\geq}(C,h)}{\log 2} \qquad (\text{resp. } j \mapsto \frac{\log \# E_j^{\leq}(C,h)}{\log 2}) \tag{6}$$

for large values of j if $h \in [h_{\min}, h_s]$ (resp. $h \in [h_s, h_{\max}]$). In practice, we fix a threshold for the correlation of the points used to compute the slope: we only keep the slope if this correlation coefficient is higher than the threshold. The impact of the choice of this threshold will be illustrated on several examples (the typical values used are $p = 0.999, 0.99, 0.95, 0.9$). From now on, the notation $\tilde{d}_f^C(h)$ will refer to this slope.

Of course, we do not know a priori the value of h_s. It is estimated as follows: we first approximate the function $\tilde{d}_f^C(h)$ using the set $E_j^{\geq}(C,h)$; let us denote this approximation by $\tilde{d}_f^{C,\geq}(h)$. Next, we do the same with $E_j^{\leq}(C,h)$ to obtain a function that we naturally denote $\tilde{d}_f^{C,\leq}(h)$. Since $\tilde{d}_f$ can be defined as the minimum of the two functions appearing in (5), the intersection of $\tilde{d}_f^{C,\geq}$ and $\tilde{d}_f^{C,\leq}$ gives an estimation of h_s.

It remains to explain how to compute an approximation of $\tilde{d}_f(h)$ using the values $\tilde{d}_f^C(h)$. It is important to understand that the main difference between the theory and the practice lies in the choice of the constant C in $\tilde{d}_f^C(h)$. Proposition 1 ensures that, at least in theory, the constant can be chosen arbitrarily. This is not true in practice because we only have access to a finite number of wavelet leaders. If the typical value of the wavelet leaders is too large (resp. too small) with respect to C, too many (resp. not enough) of them will be taken into account, so that the value $\tilde{d}_f^C(h)$ will be very different from the theoretical value $\tilde{d}_f(h)$.

Consequently, for a fixed $h > 0$, we construct the function

$$C > 0 \mapsto \tilde{d}_f^C(h)$$

to approximate the value of $\tilde{d}_f(h)$. If $h \leq h_s$ (resp. $h > h_s$) this function should be decreasing (resp. increasing). If $h \in [h_{\min}, h_{\max}]$, it should exist an interval I for which the values $\tilde{d}_f^C(h)$ with $C \in I$ are close to each other. We use a gradient descent to detect this interval [9]: the gradient is the slope of the regression line over several consecutive points (we use here 3, but taking 5 points gives the same results). We say that a stabilization is detected if several consecutive gradients are smaller than 0.01. This value may seem arbitrary (and it is indeed), but it has been chosen after both numerical considerations (what is small in regard to the implementation) and numerous experiences (on several processes such as fractional Brownian motions, Lévy processes, Poisson and binomial cascades,...). We wanted this threshold to be defined once for all independently of the considered signal. We take an interval I of minimum length $d_{\max}/2$ where $d_{\max}$ is the largest wavelet leader computed. The mean of the values $\tilde{d}_f^C(h)$ over I gives the approximation of $\tilde{d}_f(h)$.

3. Comparison of the formalisms: theoretical results

In this section, we compare from a theoretical point of view the LPM with both the WLM and the WPM. More precisely, we first show that while it is not concave, the function $\tilde{d}_f$ gives a sharper approximation of

Please cite this article in press as: C. Esser et al., A multifractal formalism for non-concave and non-increasing spectra: The leaders profile method, Appl. Comput. Harmon. Anal. (2016), http://dx.doi.org/10.1016/j.acha.2015.12.006

the spectrum of f than the WLM. We then prove that if $\tilde{d}_f$ is not with increasing-visibility, the LPM is also more efficient than the WPM on the increasing part of the spectrum.

3.1. LPM and WLM

Let us start with the following lemma which gives a connection between the function η_f and the profile $\tilde{\rho}_f$.

Lemma 2. *If $\tilde{\rho}_f$ takes the value $-\infty$ outside of a compact set of $[0,+\infty)$, then*

$$\eta_f(q) = \inf_{h\in\mathbf{R}} \{hq - \widetilde{\rho}_f(h)\} + n, \quad \forall q \in \mathbf{R}.$$

Proof. Let $h_{\min}, h_{\max} \in [0,+\infty)$ be such that $\tilde{\rho}_f$ takes the value $-\infty$ outside of $[h_{\min}, h_{\max}]$. Then

$$\inf_{h\in\mathbf{R}} \{hq - \widetilde{\rho}_f(h)\} + n = \inf_{h\in[h_{\min},h_{\max}]} \{hq - \widetilde{\rho}_f(h)\} + n.$$

Let us fix $h \in [h_{\min}, h_{\max}]$, $\delta > 0$ and $\varepsilon > 0$. From the definition of $\widetilde{\rho}_f$, there exists a subsequence $(j_m)_{m\in\mathbf{N}}$ such that

$$\#\big\{\lambda \in \Lambda_{j_m} : 2^{-(h+\varepsilon)j_m} \le d_\lambda < 2^{-(h-\varepsilon)j_m}\big\} \ge 2^{(\widetilde{\rho}_f(h)-\delta)j_m}$$

for every $m \in \mathbf{N}$. It follows that

$$\begin{aligned}
\eta_f(q) &\le \lim_{m\to+\infty} \frac{\log\left(2^{-nj_m}\sum_{\lambda\in\Lambda_{j_m}} d_\lambda^q\right)}{\log 2^{-j_m}} \\
&\le \lim_{m\to+\infty} \frac{\log\left(2^{-nj_m}2^{(\widetilde{\rho}_f(h)-\delta)j_m}2^{-(hq+\varepsilon|q|)j_m}\right)}{\log 2^{-j_m}} \\
&= n - \widetilde{\rho}_f(h) + \delta + hq + \varepsilon|q|.
\end{aligned}$$

Since $\varepsilon > 0$ and $\delta > 0$ are arbitrary, we get that

$$\eta_f(q) \le hq - \widetilde{\rho}_f(h) + n.$$

This result is valid for every $h \in [h_{\min}, h_{\max}]$ and consequently,

$$\eta_f(q) \le \inf_{h\in[h_{\min},h_{\max}]} \{hq - \widetilde{\rho}_f(h)\} + n.$$

For the other inequality, let us fix $\delta > 0$ and $\varepsilon > 0$. For every $h \in [h_{\min}, h_{\max}]$, there exist $\varepsilon_h \le \varepsilon$ and $J_h \in \mathbf{N}_0$ such that

$$\#\big\{\lambda \in \Lambda_j : 2^{-(h+\varepsilon_h)j} \le d_\lambda < 2^{-(h-\varepsilon_h)j}\big\} \le 2^{(\widetilde{\rho}_f(h)+\delta)j}$$

for every $j \ge J_h$. From the compactness of $[h_{\min}, h_{\max}]$, there exist $h_1 < \cdots < h_N$ in $[h_{\min}, h_{\max}]$, $\varepsilon_1, \ldots, \varepsilon_N \le \varepsilon$ and $J \in \mathbf{N}_0$ such that the intervals $(h_i - \varepsilon_i, h_i + \varepsilon_i)$ cover $[h_{\min}, h_{\max}]$ and

$$\#\big\{\lambda \in \Lambda_j : 2^{-(h_i+\varepsilon_i)j} \le d_\lambda < 2^{-(h_i-\varepsilon_i)j}\big\} \le 2^{(\widetilde{\rho}_f(h_i)+\delta)j}$$

for every $i \in \{1, \ldots, N\}$ and every $j \ge J$. Since $h_1 - \varepsilon_1 < h_{\min}$ and $h_N + \varepsilon_N > h_{\max}$, we can assume that

Please cite this article in press as: C. Esser et al., A multifractal formalism for non-concave and non-increasing spectra: The leaders profile method, Appl. Comput. Harmon. Anal. (2016), http://dx.doi.org/10.1016/j.acha.2015.12.006

$$2^{-(h_N+\varepsilon_N)j} \leq d_\lambda \leq 2^{-(h_1-\varepsilon_1)j}$$

for every $j \geq J$ and $\lambda \in \Lambda_j$. It follows that

$$\begin{aligned} 2^{-nj} \sum_{\lambda\in\Lambda_j} d_\lambda^q &\leq 2^{-nj} \sum_{i=1}^{N} 2^{(\widetilde{\rho}_f(h_i)+\delta)j} 2^{-(h_i q-\varepsilon_i|q|)j} \\ &\leq 2^{(\delta+\varepsilon|q|)j} \sum_{i=1}^{N} 2^{-(h_i q-\widetilde{\rho}_f(h_i)+n)j} \\ &\leq N 2^{(\delta+\varepsilon|q|)j} 2^{-\inf_{h\in\mathbf{R}}\{hq-\widetilde{\rho}_f(h)+n\}j} \end{aligned}$$

and consequently,

$$\eta_f(q) \geq \inf_{h\in\mathbf{R}} \{hq - \widetilde{\rho}_f(h)\} + n - \delta - \varepsilon|q|.$$

The numbers $\delta > 0$ and $\varepsilon > 0$ being arbitrary, we get the conclusion. □

Theorem 3. *If $\tilde{\rho}_f$ takes the value $-\infty$ outside of a compact set of $[0, +\infty)$, then $\tilde{d}_f(h) \leq d_f^\eta(h)$ for every $h \in \mathbf{R}$ and d_f^η is the concave hull of $\tilde{d}_f$.*

Proof. By definition, d_f^η is the Legendre transform of η_f. Moreover, we know from Lemma 2 that η_f is the Legendre transform of $\tilde{\rho}_f$. Using properties of this transform, we directly get that d_f^η is the concave hull of $\tilde{\rho}_f$. In particular, h_s is also the point at which d_f^η reaches its maximum. The function $\tilde{d}_f$ is the increasing hull of $\tilde{\rho}_f$ on $(-\infty, h_s]$ and its decreasing hull on $[h_s, +\infty)$ [11], hence the conclusion. □

3.2. LPM and WPM

Before comparing the LPM with the WPM, let us recall that we have

$$h_{\min} = \inf\{h \in \mathbf{R} : \nu_f(h) \geq 0\} = \inf\{h \in \mathbf{R} : \tilde{d}_f(h) \geq 0\}.$$

Theorem 4. *If $h_{\min} > 0$, then $\tilde{d}_f(h) \leq d_f^\nu(h)$ for every $h \in \mathbf{R}$. Moreover, the inequality becomes an equality on $(-\infty, h_s]$ if and only if $\tilde{d}_f$ is with increasing-visibility on $[h_{\min}, h_s]$.*

Proof. Let us fix $h \in [h_{\min}, h_s]$, $\delta > 0$, $0 < h_0 < h_{\min}$ and $\varepsilon > 0$ such that $h_0 - \varepsilon > 0$. By definition of the wavelet profile ν_f, for every $h' \leq h + \varepsilon$ there exist $\varepsilon' \leq \varepsilon$ and $J \in \mathbf{N}_0$ such that

$$\#\big\{\lambda \in \Lambda_j : |c_\lambda| \geq 2^{-(h+\varepsilon')j}\big\} \leq 2^{(\nu_f(h')+\delta)j}$$

for every $j \geq J$. Let us choose $h_1, \ldots, h_N \leq h + \varepsilon$, $\varepsilon_1, \ldots, \varepsilon_N \leq \varepsilon$ and $J \in \mathbf{N}_0$ such that the intervals $(h_i, h_i + \varepsilon_i)$ cover $[h_0, h + \varepsilon]$ and

$$\#\big\{\lambda \in \Lambda_j : |c_\lambda| \geq 2^{-(h_i+\varepsilon_i)j}\big\} \leq 2^{(\nu_f(h_i)+\delta)j}$$

for every $i \in \{1, \ldots, N\}$ and every $j \geq J$. Remark that since $h_0 < h_{\min}$, we can assume that $|c_\lambda| \leq 2^{-h_0 j}$ for every $j \geq J$. We obtain

$$\#\big\{\lambda \in \Lambda_j : d_\lambda \geq 2^{-(h+\varepsilon)j}\big\} \leq 3^n \sum_{j\leq j'\leq \frac{h+\varepsilon}{h_0} j} \#\big\{\lambda' \in \Lambda_{j'} : |c_{\lambda'}| \geq 2^{-(h+\varepsilon)j}\big\}.$$

Please cite this article in press as: C. Esser et al., A multifractal formalism for non-concave and non-increasing spectra: The leaders profile method, Appl. Comput. Harmon. Anal. (2016), http://dx.doi.org/10.1016/j.acha.2015.12.006

For every j' which appears in the sum, we have

$$h_0 \leq \frac{(h+\varepsilon)j}{j'} \leq h+\varepsilon$$

and from the covering of $[h_0, h+\varepsilon]$, there exists $i \in \{1,\dots,N\}$ such that $h_i j' \leq (h+\varepsilon)j \leq (h_i+\varepsilon_i)j'$. We get then

$$\begin{aligned}\#\big\{\lambda' \in \Lambda_{j'} : |c_{\lambda'}| \geq 2^{-(h+\varepsilon)j}\big\} &\leq \#\big\{\lambda' \in \Lambda_{j'} : |c_{\lambda'}| \geq 2^{-(h_i+\varepsilon_i)j'}\big\} \\ &\leq 2^{(\nu_f(h_i)+\delta)j'} \\ &\leq 2^{(\nu_f(h_i)+\delta)\frac{h+\varepsilon}{h_i}j}\end{aligned}$$

and consequently,

$$\#\big\{\lambda \in \Lambda_j : d_\lambda \geq 2^{-(h+\varepsilon)j}\big\} \leq 3^n \left(\left(\frac{h+\varepsilon}{h_0}-1\right)j+1\right) 2^{j(h+\varepsilon)\sup_{h'\in(0,h+\varepsilon]}\frac{\nu_f(h')+\delta}{h'}}.$$

It follows that

$$\limsup_{j\to+\infty} \frac{\log \#\big\{\lambda \in \Lambda_j : d_\lambda \geq 2^{-(h+\varepsilon)j}\big\}}{\log 2^j} \leq \sup_{h'\in(0,h+\varepsilon]} (\nu_f(h')+\delta)\frac{h+\varepsilon}{h'}.$$

Taking the limit as $\varepsilon \to 0^+$ and using the right-continuity of ν_f, we get

$$\tilde{d}_f(h) \leq h \sup_{h'\in(0,h]} \frac{\nu_f(h')+\delta}{h'} \leq h \sup_{h'\in(0,h]} \frac{\nu_f(h')}{h'} + \delta\frac{h}{h_{\min}}.$$

Since $\delta > 0$ is arbitrary, we obtain the first part of the proposition. Moreover, we have

$$\nu_f(h) \leq \tilde{d}_f(h) \leq h \sup_{h'\in(0,h]} \frac{\nu_f(h')}{h'}$$

for every $h \in [h_{\min}, h_s]$, which leads to the conclusion. □

4. Numerical simulations on theoretical examples

In this section, the LPM (implemented as explained in section 2.5) is compared with both the WLM [8] and the WPM [9] on several numerical simulations based on theoretical examples. We show that in most cases, the LPM is better than the WPM and that it works in a more general context than the WLM. We begin with the simple case of a family of monofractal functions, before dealing with multifractal functions associated with both concave and non-concave spectra.

4.1. Monofractal example: the fractional Brownian motion

A classical monofractal process is the fractional Brownian motion [20]. It is the unique Gaussian stochastic process that is self-similar with stationary increments and it depends on a parameter $H \in (0,1)$, called the *Hurst index*. The walk of a fractional Brownian motion of parameter H is continuous, nowhere differentiable and the associated Hölder exponent is equal to H almost surely [21].

These motions model many monofractal phenomena [20,22–24]. In Fig. 1, we have used the algorithm of Wood–Chan [25] to simulate some fractional Brownian motions. Let us recall that if H is equal to 0.5 (resp.

Please cite this article in press as: C. Esser et al., A multifractal formalism for non-concave and non-increasing spectra: The leaders profile method, Appl. Comput. Harmon. Anal. (2016), http://dx.doi.org/10.1016/j.acha.2015.12.006

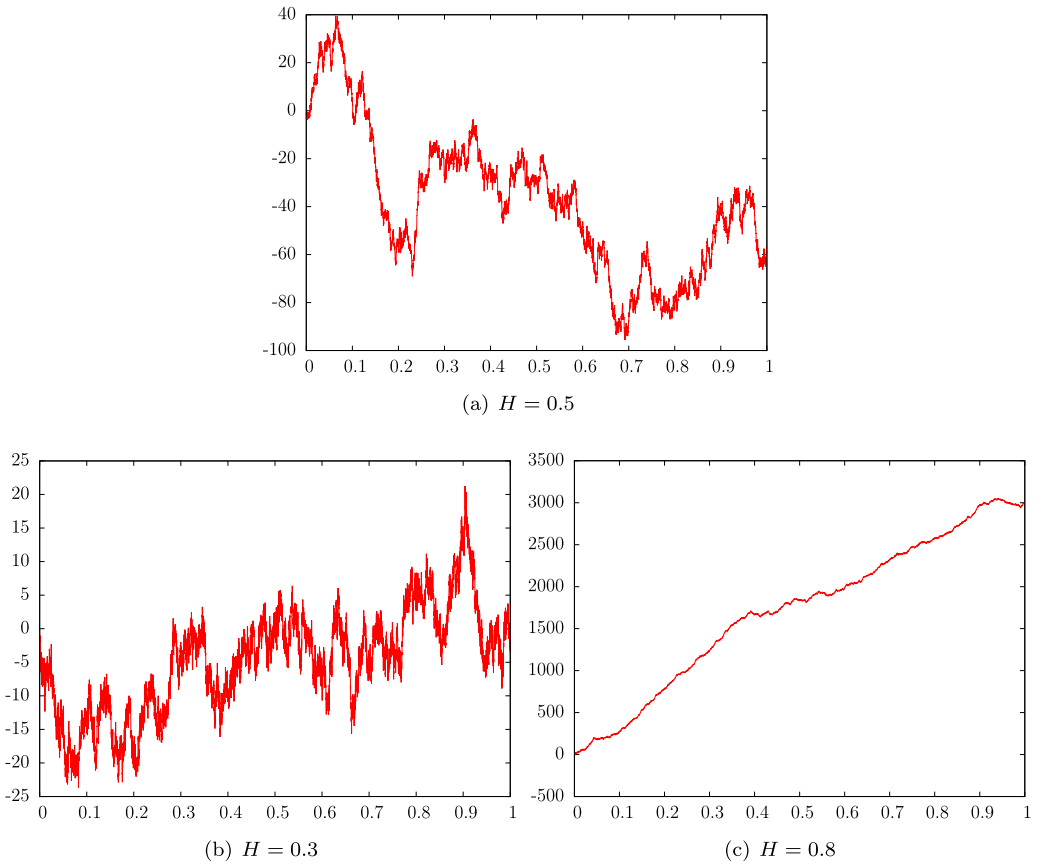

(a) $H = 0.5$

(b) $H = 0.3$

(c) $H = 0.8$

Fig. 1. Fractional Brownian motions with parameter H.

smaller than 0.5, larger than 0.5) the increments are independent (resp. negatively correlated, positively correlated).

As a first illustration, we have computed the spectrum of a classical Brownian motion (i.e. a fractional Brownian motion with $H = 0.5$). In Fig. 2, several examples of functions $C \mapsto \tilde{d}_f^{C,\geq}(h)$ are represented for $h \leq 0.5$. In Figs. 2(a), 2(b) and 2(c), one can see that the graphs do not stabilize for $C > d_{\max}$ or are less stable than in Fig. 2(d) (we recall that $d_{\max}$ is defined as the largest computed wavelet leader). Let us remark that the stabilization for $C < d_{\max}$ is due to the fact that we have only a finite number of coefficients. Therefore, almost every wavelet leader is taken into account in the computation of $\#E_j^{\geq}(C,h)$. Thus, this first stabilization is never relevant.

In Fig. 3, several functions $C \mapsto \tilde{d}_f^{C,\leq}(h)$ are represented for $h > 0.5$. The graphs do not stabilize and the larger the constant C is, the closer to 1 the function is. Remark that these graphs always reach the value 1 because for large C, every wavelet leader is taken into account in the computation of $\#E_j^{\leq}(C,h)$, so that this last stabilization is not relevant.

In order to limit the human interaction, we use the method explained in Section 2.5 to approximate h_s, i.e. H in this case. In Fig. 4, we have represented the spectrum of a Brownian motion obtained with the three wavelet-based methods. For the LPM, we use the threshold $p = 0.99$ to compute the functions defined in (6). One can see that the LPM gives better results than the WPM. For the WLM, the function η (defined in (3)) seems linear. The usual way to proceed in this case is to define the Hölder exponent as the slope of η; indeed, estimating a multifractal spectrum leads to inaccurate results here, as the support of the so-computed spectrum is far too big (Fig. 4(c)). To detect more precisely the value of H, one considers the slope of η computed on several intervals [26]. The Hölder exponent is the mean of these slopes, the standard

Please cite this article in press as: C. Esser et al., A multifractal formalism for non-concave and non-increasing spectra: The leaders profile method, Appl. Comput. Harmon. Anal. (2016), http://dx.doi.org/10.1016/j.acha.2015.12.006

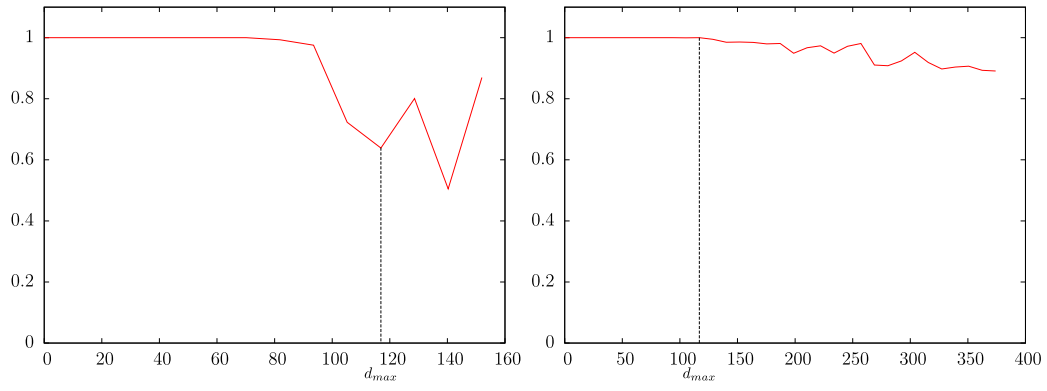

(a) $h = 0.4$ (b) $h = 0.48$

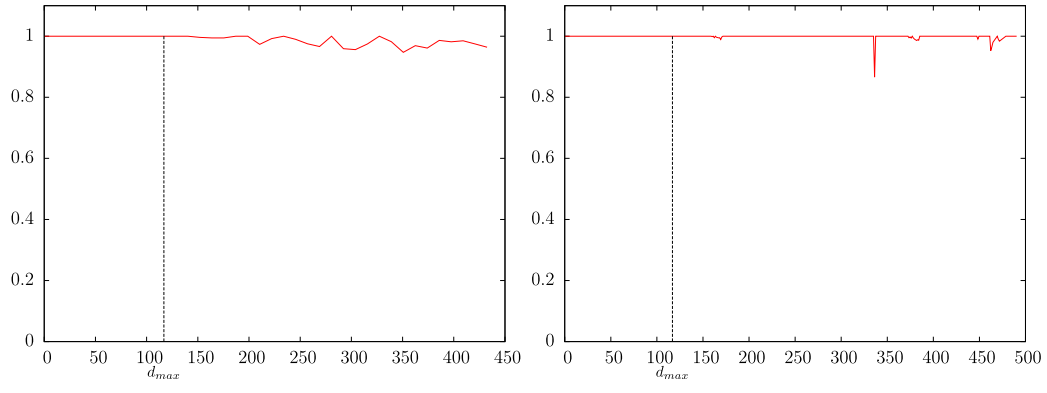

(c) $h = 0.49$ (d) $h = 0.50$

Fig. 2. Functions $C \mapsto \tilde{d}_f^{C,\geq}(h)$ for the increasing part of the spectrum of a Brownian motion.

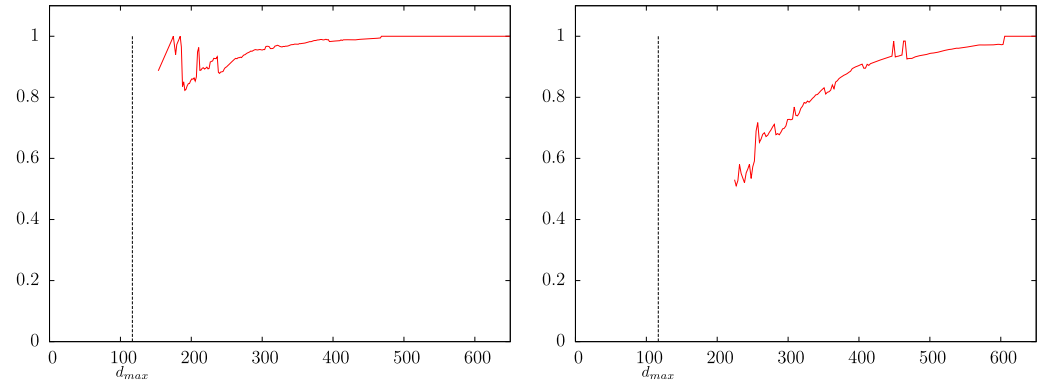

(a) $h = 0.51$ (b) $h = 0.52$

Fig. 3. Functions $C \mapsto \tilde{d}_f^{C,\leq}(h)$ for the decreasing part of the spectrum of a Brownian motion.

deviation giving error bars. The result is shown in Fig. 4(d). If one concludes from the behavior of η that the function is monofractal, the WLM is very competitive, but it is also the worse method without this conjecture.

For a fixed size 2^j ($2^{11} \leq 2^j \leq 2^{20}$) and a fixed parameter H ($H \in [0.1, 0.9]$), we have simulated 100 fractional Brownian motions. Fig. 5 shows for every j, the mean and the box plot of the distances between the Hölder exponent detected and H (i.e. the absolute value of their difference) for the simulations of size 2^j.

Please cite this article in press as: C. Esser et al., A multifractal formalism for non-concave and non-increasing spectra: The leaders profile method, Appl. Comput. Harmon. Anal. (2016), http://dx.doi.org/10.1016/j.acha.2015.12.006

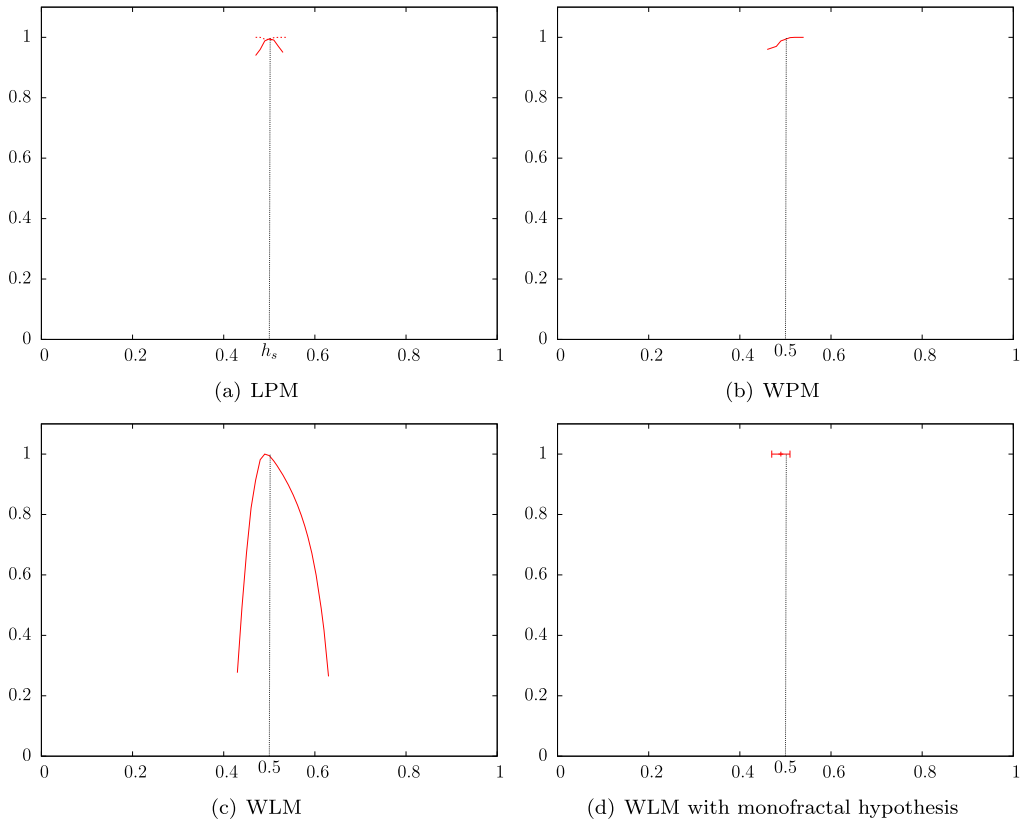

Fig. 4. Spectrum of a Brownian motion obtained with (a) the LPM (the dotted lines represent the parts of the functions defined in (5) that are not taken into account to define the spectrum), (b) the WPM, (c) the WLM and (d) the WLM with the monofractal hypothesis (if the linear behavior of the function η leads to the conclusion that the studied function is monofractal (this is the monofractal hypothesis), the usual way to estimate the Hölder exponent is to compute the slope over different intervals, the mean of these slopes defining the exponent and the standard deviation leading to error bars).

For sizes between 2^{15} and 2^{20}, the three methods give similar results, with a slight advantage for the LPM and the WPM for large sizes. For small sizes, the WPM becomes significantly less accurate than the two other methods. Let us recall that it is the only method which directly uses the wavelet coefficients; the other two methods use the wavelet leaders. Large wavelet leaders mark off the singularities of the function, while this has not to be true for the wavelet coefficients. Heuristically, the statistics based on the wavelet coefficients should be more irrelevant for studying singularities [6].

4.2. Multifractal examples

The first multifractal example that we will consider is the Lévy process. It is for example used in the field of financial modeling [27]. It is a stochastic process with independent and stationary increments that is right-continuous and admits almost surely a left limit at all points. It is associated to an index $\beta \in [0, 2]$, called the *Blumenthal and Getoor lower index*, that governs the multifractal properties of the process. Any Lévy process can be decomposed into the sum of a (possibly vanishing) Brownian part and an independent pure jumps process.

The multifractal properties of the Lévy process have been studied in [28]. If the process has no Brownian part, the Hölder spectrum is almost surely equal to

$$d_f(h) = \beta h$$

Please cite this article in press as: C. Esser et al., A multifractal formalism for non-concave and non-increasing spectra: The leaders profile method, Appl. Comput. Harmon. Anal. (2016), http://dx.doi.org/10.1016/j.acha.2015.12.006

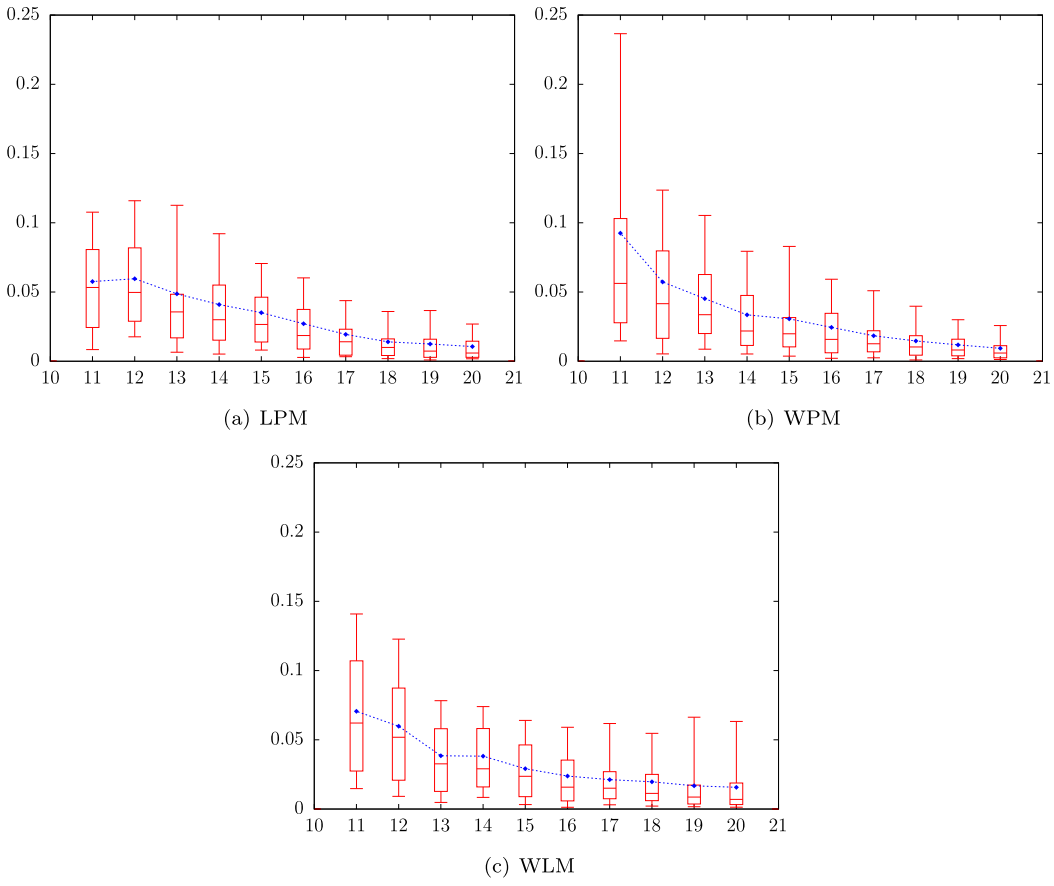

Fig. 5. Functions that represent for every j, the box plot of the distances between the Hölder exponent detected and H for 100 simulations of size 2^j of fractional Brownian motions. The mean of these distances is also represented (in blue). (For interpretation of the references to color in this figure legend, the reader is referred to the web version of this article.)

for all $h \in [0, 1/\beta]$. On the other hand, if the process has a Brownian part, the associated Hölder spectrum is almost surely equal to

$$d_f(h) = \begin{cases} \beta h & \text{if } h \in [0, 1/2) \\ 1 & \text{if } h = 1/2 \end{cases}.$$

To simulate a Lévy process without Brownian part, the algorithm described in [29] is used. A Brownian motion is then added to create a Lévy process with a Brownian part. In Fig. 6, simulations of Lévy processes are represented.

First, let us study the case of a Lévy process without Brownian part associated to the index $\beta = 1.3$. Let us recall that in order to approximate the spectrum with $h > 0$, we first build the function $C > 0 \mapsto \tilde{d}_f^{C,\geq}(h)$. If there is a stabilization, the mean of the ordinates corresponding to this stabilization defines the approximation. In Fig. 7, several examples are represented. For $h = 0.38$ (Fig. 7(a)), we have a stabilization, but for $h = 0.65$ (Fig. 7(b)) the function is more unstable for large C. The reason is that the number of wavelet leaders taken into account in the computation of $\tilde{d}_f^{C,\geq}(h)$ increases with h. To avoid this problem, a simple solution is to raise the threshold for the correlation (see section 2.5) in order to only keep the points which are strongly correlated. By default, this threshold is set to 0.99; in Fig. 7(c), we have only kept the points with a correlation larger than 0.999. One can notice that in this case the function stabilizes.

The use of the formula for the decreasing part of the spectrum is illustrated in Fig. 8. One can see that the function $C > 0 \mapsto d_f^{C,\leq}(h)$ has no stabilization for $h > 1/\beta$.

Please cite this article in press as: C. Esser et al., A multifractal formalism for non-concave and non-increasing spectra: The leaders profile method, Appl. Comput. Harmon. Anal. (2016), http://dx.doi.org/10.1016/j.acha.2015.12.006

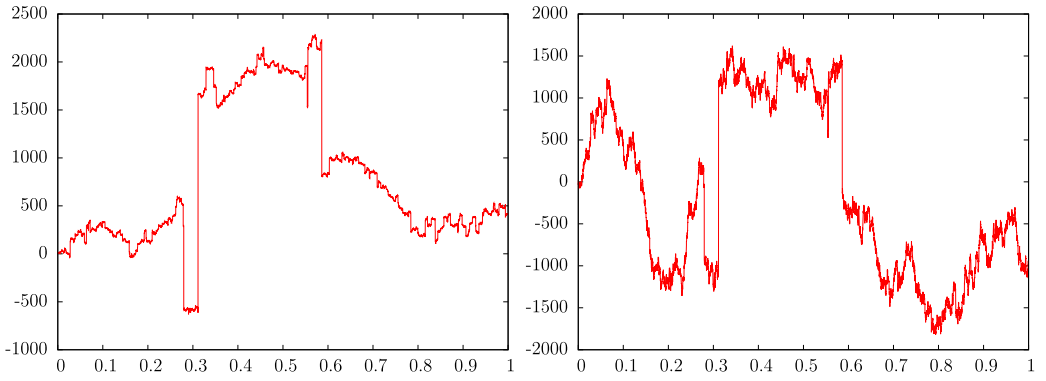

(a) Lévy process without Brownian part (b) Lévy process with a Brownian part

Fig. 6. Lévy processes with $\beta = 1.3$.

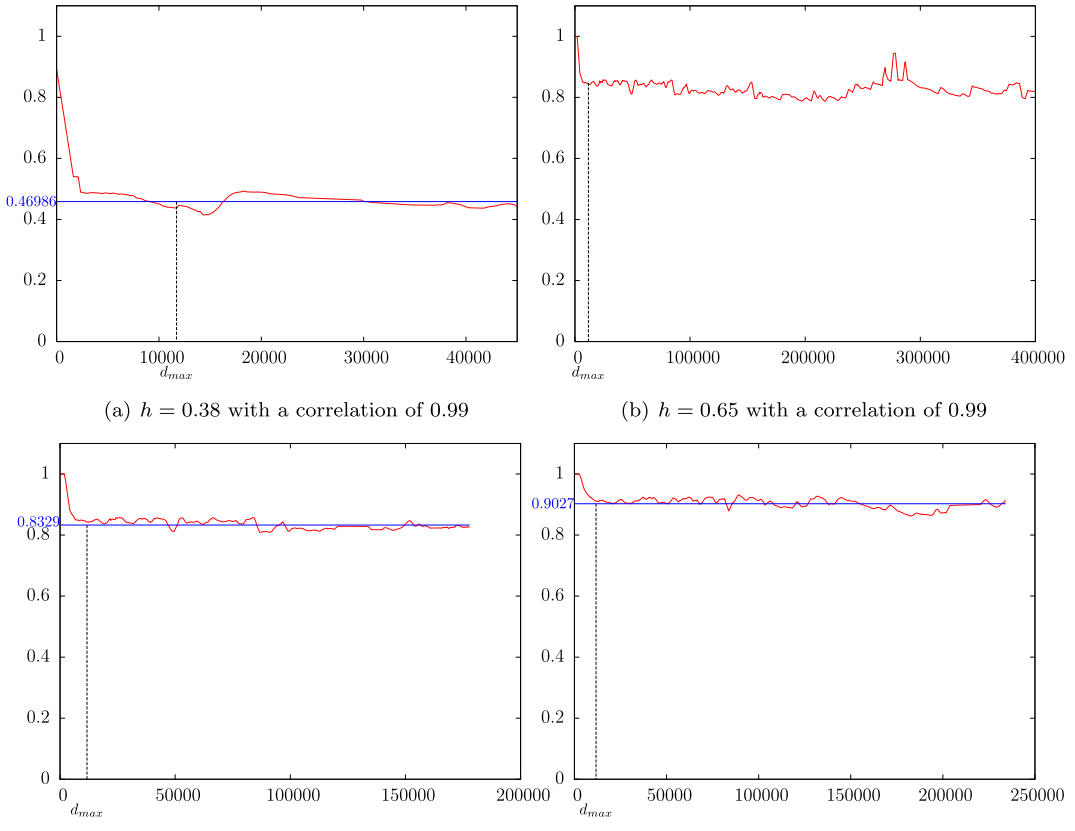

(a) $h = 0.38$ with a correlation of 0.99 (b) $h = 0.65$ with a correlation of 0.99

(c) $h = 0.65$ with a correlation of 0.999 (d) $h = 0.70$ with a correlation of 0.999

Fig. 7. Functions $C \mapsto \tilde{d}_f^{C,\geq}(h)$ for the increasing part of the spectrum of a Lévy process ($\beta = 1.3$).

The theoretical spectrum is compared with the spectra obtained with the LPM, the WPM and the WLM in Fig. 9. First, we see that the WLM tends to determine a strictly concave spectrum while the LPM and the WPM fit the theoretical spectrum better. Secondly, the LPM and the WPM do not detect the spectrum for small h. These two methods are based on the same ideas: to determine the behavior of the number of coefficients that are greater than 2^{-hj} across scales j. For small values of h, there are not enough remaining coefficients, so that it is very difficult to have an acceptable stabilization. However, the contribution of the wavelet leaders is not negligible. They can determine a stabilization for smaller h than the wavelet coefficients.

Please cite this article in press as: C. Esser et al., A multifractal formalism for non-concave and non-increasing spectra: The leaders profile method, Appl. Comput. Harmon. Anal. (2016), http://dx.doi.org/10.1016/j.acha.2015.12.006

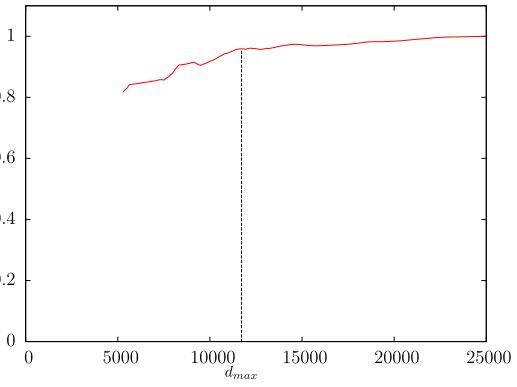

(a) $h = 0.78$ with a correlation of 0.99

Fig. 8. Function $C \mapsto \tilde{d}_f^{C,\leq}(h)$ for the decreasing part of the spectrum of a Lévy process ($\beta = 1.3$).

Table 1
Mean values for the smallest h detected for a Lévy process of size 2^j ($\beta = 1.3$).

$j = 20$	LPM	WPM
$p = 0.99$	0.31	0.37
$p = 0.95$	0.25	0.31
$p = 0.9$	0.19	0.24

$j = 15$	LPM	WPM
$p = 0.99$	0.44	0.52
$p = 0.95$	0.37	0.45
$p = 0.9$	0.34	0.41

For a fixed size 2^j ($2^{12} \leq 2^j \leq 2^{20}$), we simulate 50 Lévy process without Brownian part ($\beta = 1.3$). For a fixed j, we compute the root-mean-square deviation (RMSE) of each simulation of size 2^j. The mean and the box plot of these RMSE are represented in Fig. 10. The three different methods (LPM, WPM and WLM) are also compared and for the LPM and the WPM, the impact of the threshold p for the correlation of the points in formula (6) is studied. We see that the LPM and the WPM are clearly better than the WLM. Besides, we remark that the LPM and the WPM are more precise for $p = 0.99$. However, as illustrated in Table 1, the larger p is, the larger the smallest detected value of h is.

In conclusion, in this example, both the LPM and the WPM cannot determine the spectrum for small h but when the methods detect a spectrum, it is more accurate than the WLM. Moreover, thanks to the specificity of the wavelet leaders, the LPM is better than the WPM.

Now, let us study a Lévy process with a Brownian part; let us recall that its spectrum is non-concave. The theoretical spectrum is compared with the spectra obtained with the LPM, the WPM and the WLM in Fig. 11. By definition, the WLM cannot lead to non-concave spectra: It can only determine the concave hull of a spectrum. We see that the LPM and the WPM are close to the theoretical spectrum and detect the non-concave part of the spectrum. The discussion for the small values of h and the size of the simulation is the same as in the case of a Lévy process without Brownian part.

The last example we consider is a signal whose spectrum has a non-increasing part; it is based on the notion of multiplicative cascades. This notion is very important since it models many phenomena, including turbulence. The simplest case is given by the binomial cascade.

Definition 2. The binomial cascade of parameter $p \in (0,1)$ is the only Borel measure μ defined on $[0,1]$ such that

$$\mu\Big(\Big[\sum_{k=1}^{n} \frac{\varepsilon_k}{2^k}, \sum_{k=1}^{n} \frac{\varepsilon_k}{2^k} + \frac{1}{2^n}\Big)\Big) = p^{\sum_{k=1}^{n} \varepsilon_k} (1-p)^{n - \sum_{k=1}^{n} \varepsilon_k},$$

for all $n \in \mathbf{N}$ and $\varepsilon_k \in \{0,1\}$ ($k \in \{1, \ldots, n\}$).

Please cite this article in press as: C. Esser et al., A multifractal formalism for non-concave and non-increasing spectra: The leaders profile method, Appl. Comput. Harmon. Anal. (2016), http://dx.doi.org/10.1016/j.acha.2015.12.006

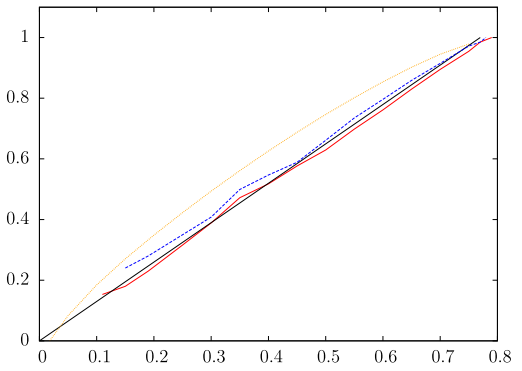

(a) Simulations of size 2^{20}

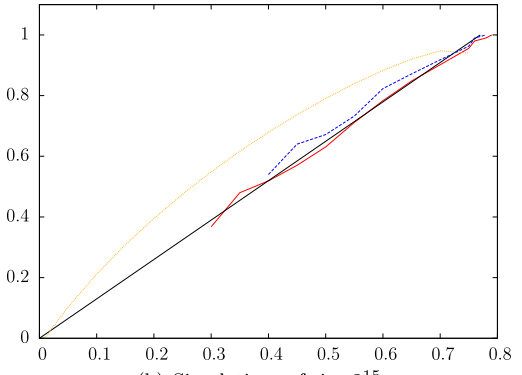

(b) Simulations of size 2^{15}

Fig. 9. Spectrum of the Lévy process without Brownian part ($\beta = 1.3$). Black (resp. red, blue and orange) theoretical (resp. LPM, WPM, WLM) spectrum. The results are obtained with 50 simulations. (For interpretation of the references to color in this figure legend, the reader is referred to the web version of this article.)

Following a general framework proposed by Barral and Seuret [30], let us construct a function f by prescribing its wavelet coefficients in a given wavelet basis as follows: for every λ, we set $c_\lambda = \mu(\lambda)$. We will say that the function f is a binomial cascade of parameter p. Let us mention that f and μ have the same multifractal properties.

The Hölder spectrum of a binomial cascade of parameter $p \in (0, 1/2)$ is

$$d_f(h) = -\big(\alpha \log_2 \alpha + (1-\alpha)\log_2(1-\alpha)\big),$$

where

$$\alpha = \frac{h + \log_2(1-p)}{\log_2(1-p) - \log_2 p},$$

for all $h \in [-\log_2(1-p), -\log_2 p]$ (for a proof, see e.g. [31]).

In [32], the method of *threshold of order* $\gamma > 0$ was introduced. It consists in replacing the wavelet coefficients c_λ by

$$c_\lambda^t = c_\lambda \mathbf{1}_{|\cdot| \geq 2^{-\gamma j}}(c_\lambda).$$

In the case of a binomial cascade f of parameter $p \in (0, 1/2)$, if f^t is the function obtained after a threshold of order γ, then the Hölder spectrum of f^t is non-concave [32]. More precisely, denote by $\omega_t : [\gamma, -\log_2(p)] \to (0, +\infty)$ the increasing function

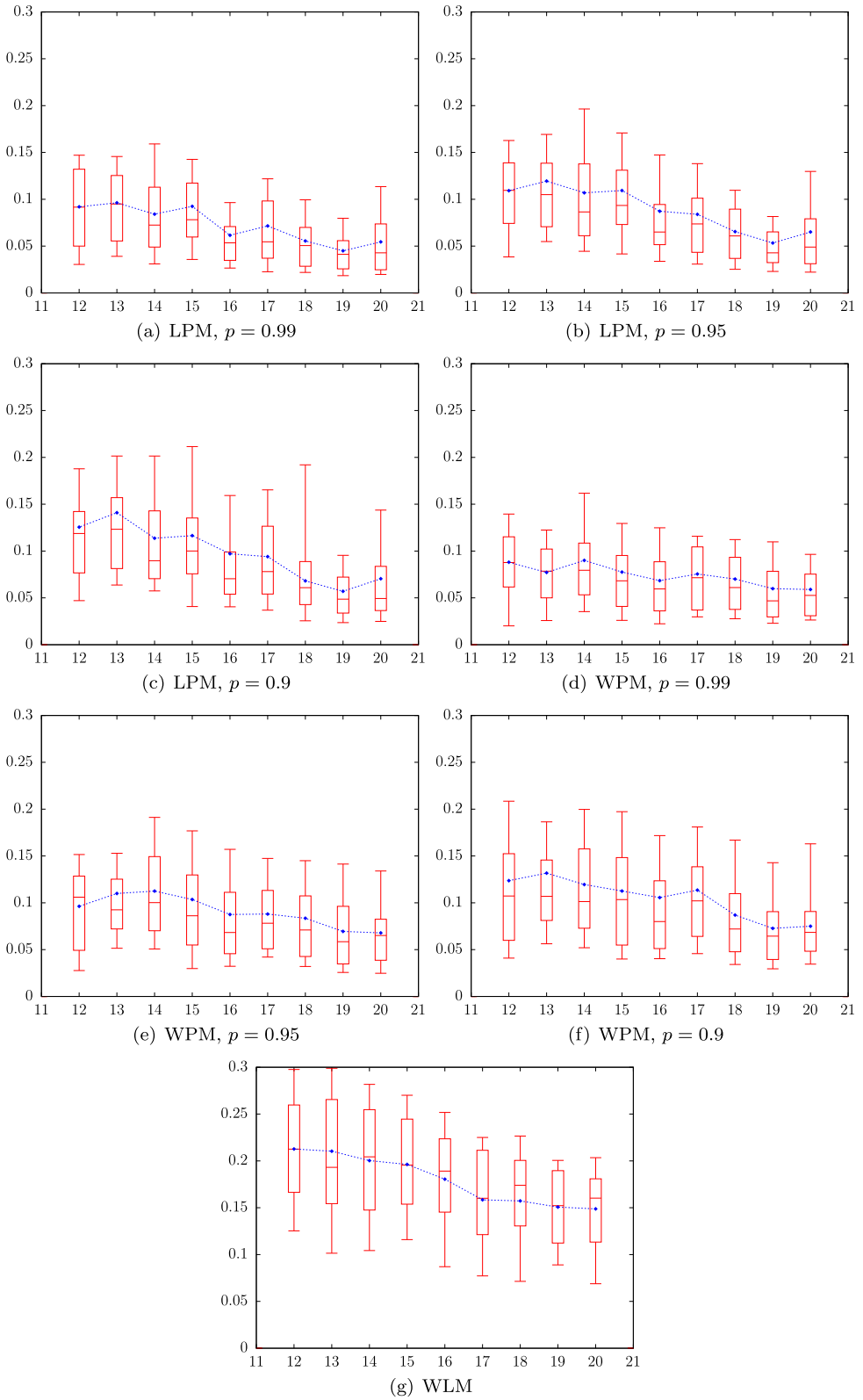

Fig. 10. Functions that represent for every j, the box plot of the RMSE. The mean of these RMSE is also represented (in blue). The value p represents the threshold for the correlation of the points in formula (6). (For interpretation of the references to color in this figure legend, the reader is referred to the web version of this article.)

Please cite this article in press as: C. Esser et al., A multifractal formalism for non-concave and non-increasing spectra: The leaders profile method, Appl. Comput. Harmon. Anal. (2016), http://dx.doi.org/10.1016/j.acha.2015.12.006

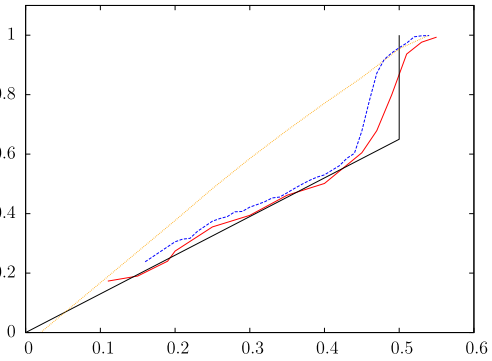

Fig. 11. Spectrum of a Lévy process with a Brownian part ($\beta = 1.3$). Black (resp. red, blue and orange) theoretical spectrum (resp. LPM, WPM, WLM). The results are obtained with 50 simulations of size 2^{20}. (For interpretation of the references to color in this figure legend, the reader is referred to the web version of this article.)

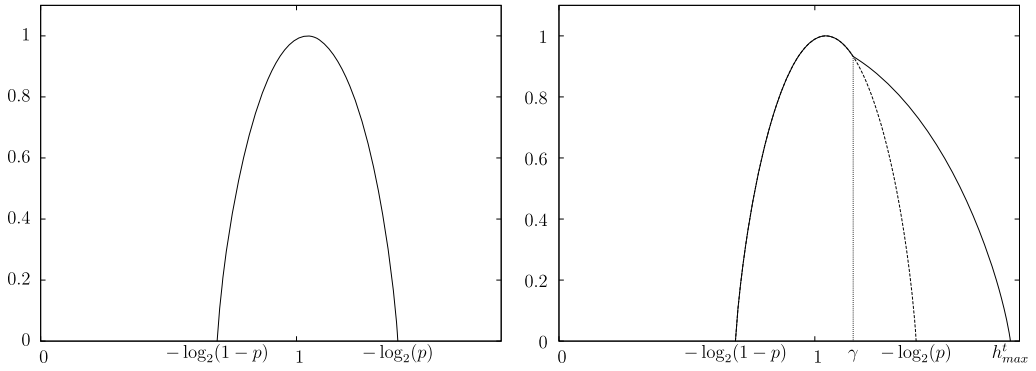

Fig. 12. Theoretical spectrum of a binomial cascade of parameter $p = 0.38$ (left) and its threshold of order $\gamma = 1.15$ (right).

$$u \mapsto \gamma \frac{u + \log_2(1-p)}{\gamma + \log_2(1-p)}$$

and by $h^t_{\max} = \omega_t(-\log_2 p)$; if $\gamma \in [-\log_2(1-p), -\log_2 p]$, the Hölder spectrum of f^t is equal to

$$d_{f^t}(h) = \begin{cases} d_f(h) & \text{if } h \in [-\log_2(1-p), \gamma], \\ d_f(\omega_t^{-1}(h)) & \text{if } h \in (\gamma, h^t_{\max}], \\ -\infty & \text{otherwise.} \end{cases}$$

This is illustrated in Fig. 12.

The theoretical spectra of a binomial cascade and of its threshold are compared with the spectra obtained with the LPM and the WLM in Fig. 13. The WPM is not illustrated here since it can only detect the increasing part of spectra. In the two examples, the LPM underestimates the theoretical spectrum but it detects the non-concave part of the spectrum of the threshold function. The WLM does not detect this non-concave part. However, one can argue from Fig. 13 that the spectrum obtained with the LPM seems also non-concave where it is theoretically concave. This is due to the fact that the threshold binomial cascade is numerically very badly behaved. As shown in Fig. 14, this non-concave aspect disappears as one increases the number of points; the spectrum is also closer to the theoretical one. Here again, the part of the spectrum corresponding to the smallest values of h cannot be detected.

While studying the function $C \mapsto \tilde{d}_f^{C,\leq}(h)$ with $h > \gamma = 1.15$ for the approximation of the decreasing part of the threshold cascade, we have noticed two stabilizations. The highest corresponds to the theoretical

Please cite this article in press as: C. Esser et al., A multifractal formalism for non-concave and non-increasing spectra: The leaders profile method, Appl. Comput. Harmon. Anal. (2016), http://dx.doi.org/10.1016/j.acha.2015.12.006

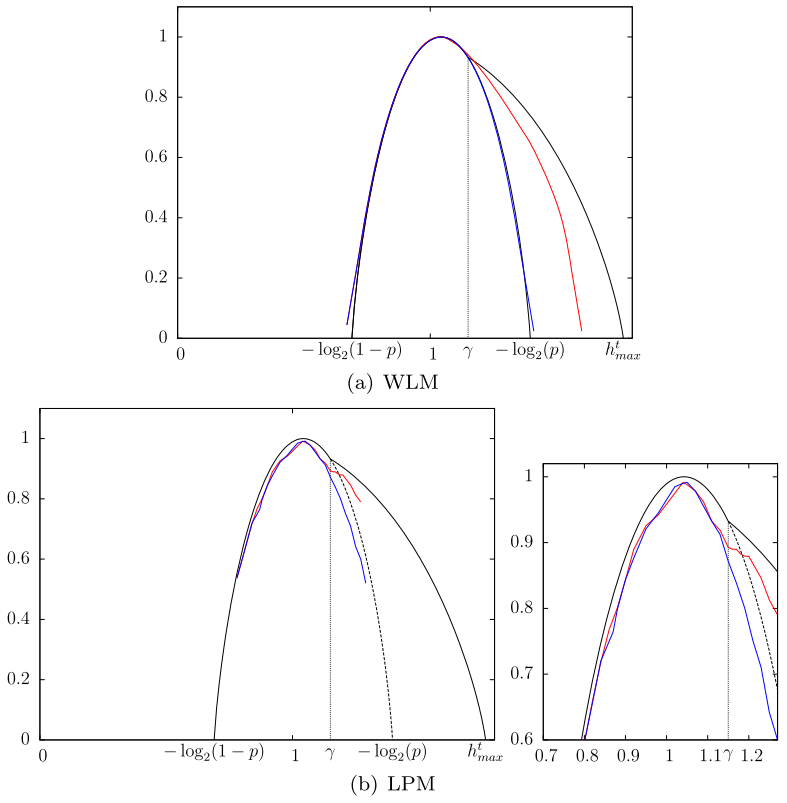

Fig. 13. Blue (resp. red) spectrum of a binomial cascade of parameter $p = 0.38$ (resp. its threshold of order $\gamma = 1.15$). The results are obtained with signals of size 2^{20}. (For interpretation of the references to color in this figure legend, the reader is referred to the web version of this article.)

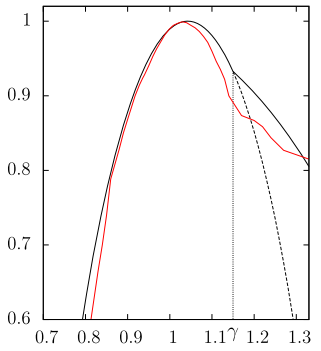

Fig. 14. Spectrum of a threshold cascade of parameter $p = 0.38$ and $\gamma = 1.15$ with the LPM. The results are obtained with a signal of size 2^{60}.

value, while the smallest corresponds to the cascade without the threshold. In Fig. 15, several examples are represented to compare the detected stabilizations for a cascade and for its threshold. The presence of two stabilizations can be explained as a numerical phenomenon. The threshold replaces the small coefficients by 0. So, the value of $\tilde{d}_f^{C,\leq}(h)$ (which depends on the number of coefficients smaller than $C2^{-hj}$) for small C reflects this modification. On the opposite, the value of $\tilde{d}_f^{C,\leq}(h)$ for large C is less affected by this change and allows to detect the presence of the original cascade. In Fig. 16, the values of the smallest stabilizations are represented.

These last examples lead to the conclusion that the LPM provides additional information with respect to the WLM. For a binomial cascade, the LPM confirms that the spectrum is strictly concave. In this case,

Please cite this article in press as: C. Esser et al., A multifractal formalism for non-concave and non-increasing spectra: The leaders profile method, Appl. Comput. Harmon. Anal. (2016), http://dx.doi.org/10.1016/j.acha.2015.12.006

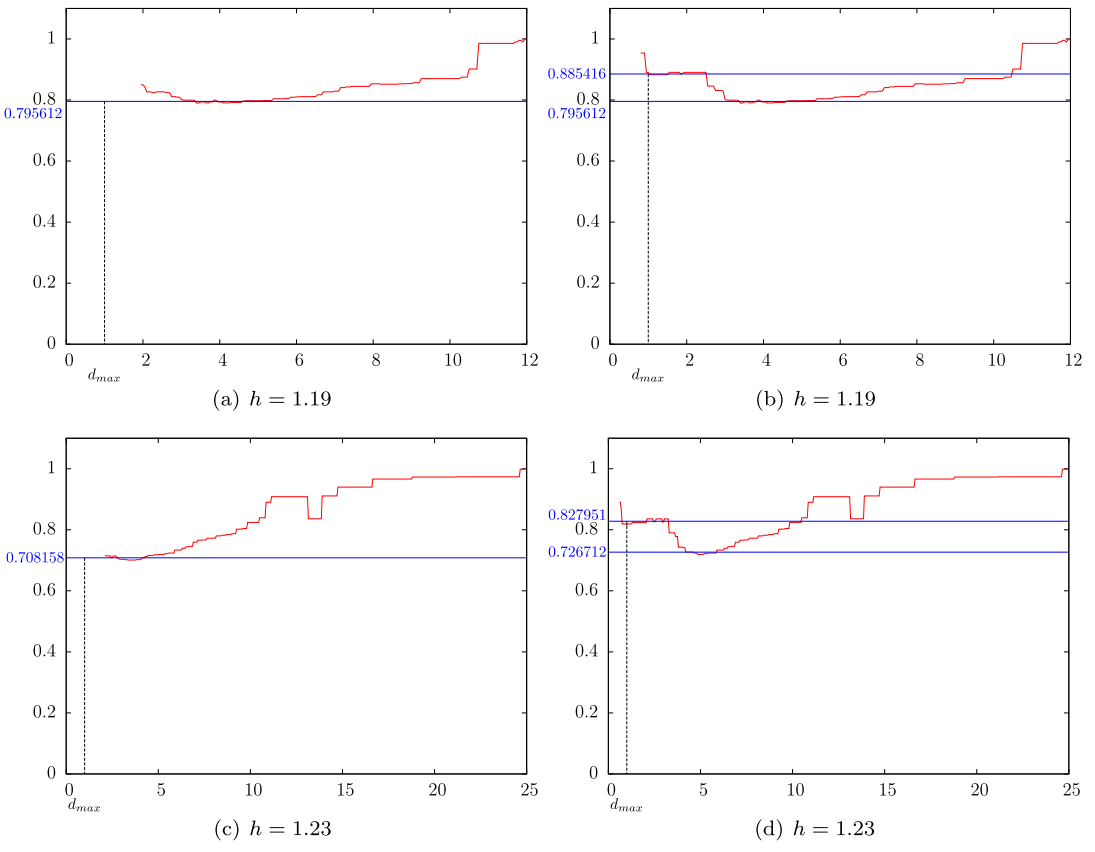

Fig. 15. Function $C \mapsto \tilde{d}_f^{C,\leq}(h)$ for the decreasing part of the spectrum of a cascade of parameter $p = 0.38$ (left) and its threshold of order $\gamma = 1.15$ (right).

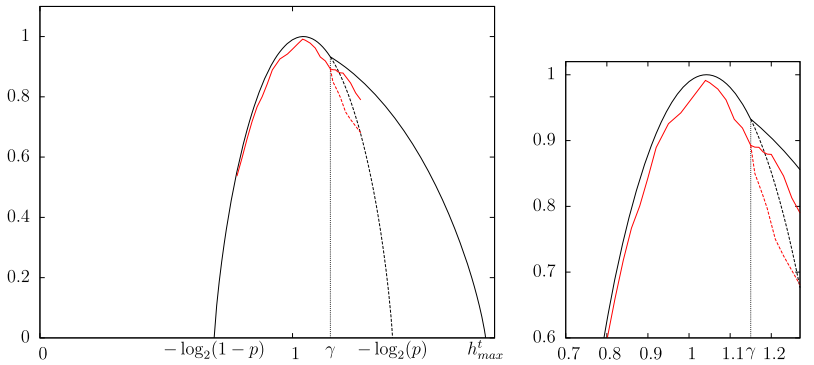

Fig. 16. Spectrum of a cascade of parameter $p = 0.38$ with a threshold of order $\gamma = 1.15$. Black (resp. red) theoretical spectrum (resp. LPM). Dotted black (resp. red) theoretical spectrum of a cascade of parameter $p = 0.38$ (resp. the smallest stabilization detected with the LPM). (For interpretation of the references to color in this figure legend, the reader is referred to the web version of this article.)

the WLM detects the theoretical spectrum. For the signal obtained after a threshold, the LPM indicates the presence of a non-concave part. The spectrum obtained with the WLM is necessarily not correct: it gives only the concave hull of the theoretical spectrum. Thus, the LPM gives additional information about the theoretical spectrum. Besides, the LPM detects the presence of two phenomena in the signal: the cascade and the cascade with a threshold. This last fact is very interesting in practice and must be thorough.

Please cite this article in press as: C. Esser et al., A multifractal formalism for non-concave and non-increasing spectra: The leaders profile method, Appl. Comput. Harmon. Anal. (2016), http://dx.doi.org/10.1016/j.acha.2015.12.006

5. Conclusion

From a theoretical point of view, we have shown that the LPM is more efficient than the WLM: the WLM only gives the concave hull of the spectrum obtained with the LPM. Concerning the WPM, a similar result holds: the WPM only leads to the increasing-visibility-part of the spectrum given by the LPM.

On the practical playground, these results have been confirmed. First, all the methods behave in the same way for monofractal signals, as illustrated for fractional Brownian motions. Concerning multifractal signals, as illustrated with Lévy processes, the WLM tends to give strictly concave estimations, so that the LPM appears to be more precise. However, as shown for the Lévy process and the binomial cascade, the LPM cannot detect the part of spectra corresponding to the smallest values of h. The same problem is observed with the WPM and is even worse, since larger parts are missed. Of course, the WPM cannot detect the decreasing parts of spectra.

As a conclusion, the LPM is a method that allows the computation of non-concave and non-increasing spectra. Both the WLM and the LPM are complementary: the first approach relies on the assumption that the researched spectrum is concave. Such a hypothesis can be tested with the LPM. Also, the WLM allows to estimate the earlier part of the spectrum (corresponding to the smallest values of h), which is not the case with the LPM. The size of the analyzed signal is more critical for the LPM. If the number of data is not large enough, it can be dubious to assert that a spectrum computed via the LPM is non-concave, since numerical effects can be involved; the same well-known problem is met when studying signals that are possibly monofractal.

Acknowledgments

The authors would like to thank Stéphane Jaffard for the discussions that have led to this manuscript. The first author is supported by a grant of the Fonds De La Recherche Scientifique - FNRS.

References

[1] G. Parisi, U. Frisch, On the singularity structure of fully developed turbulence, in: Turbulence and Predictability in Geophysical Fluid Dynamics, 1985, pp. 84–87.
[2] K. Falconer, The Geometry of Fractal Sets, Cambridge University Press, 1986.
[3] A. Arneodo, G. Grasseau, M. Holschneider, Wavelet transform of multifractals, Phys. Rev. Lett. 61 (1988) 2281–2284.
[4] S. Jaffard, Multifractal formalism for functions part I: results valid for all functions, SIAM J. Math. Anal. 28 (1997) 944–970.
[5] J.-F. Muzy, E. Bacry, A. Arneodo, Multifractal formalism for fractal signals: the structure function approach versus the wavelet-transform modulus-maxima method, Phys. Rev. E 47 (1993) 875–884.
[6] S. Jaffard, Wavelet techniques in multifractal analysis, fractal geometry and applications: a jubilee of Benoit Mandelbrot, Proc. Sympos. Pure Math. 72 (2004) 91–151.
[7] S. Jaffard, Beyond Besov spaces part 2: oscillation spaces, Constr. Approx. 21 (2005) 29–61.
[8] S. Jaffard, S. Nicolay, Pointwise smoothness of space-filling functions, Appl. Comput. Harmon. Anal. 26 (2009) 181–199.
[9] T. Kleyntssens, C. Esser, S. Nicolay, A multifractal formalism based on the S^ν spaces: from theory to practice, submitted for publication.
[10] J.-M. Aubry, S. Jaffard, Random wavelet series, Comm. Math. Phys. 227 (2002) 483–514.
[11] F. Bastin, C. Esser, S. Jaffard, Large deviation spectra based on wavelet leaders, Rev. Mat. Iberoam., to appear.
[12] J. Barral, P. Gonçalves, On the estimation of the large deviations spectrum, J. Stat. Phys. 144 (2011) 1256–1283.
[13] I. Daubechies, Ten Lectures on Wavelets, CBMS-NSF Regional Conference Series in Applied Mathematics, 1992.
[14] Y. Meyer, D. Salinger, Wavelets and Operators, vol. 1, Cambridge University Press, 1995.
[15] S. Mallat, A Wavelet Tour of Signal Processing, Academic Press, 1999.
[16] W. Dahmen, S. Prössdorf, R. Schneider, Wavelet approximation methods for pseudodifferential equations: I stability and convergence, Math. Z. 215 (1994) 583–620.
[17] S. Jaffard, Beyond Besov spaces part 1: distributions of wavelet coefficients, J. Fourier Anal. Appl. 10 (2004) 221–246.
[18] D. Maman, S. Seuret, Fixed points for multifractal spectrum application, Constr. Approx., to appear, http://dx.doi.org/10.1007/s00365-015-9317-z.
[19] J.-M. Aubry, F. Bastin, S. Dispa, S. Jaffard, Topological properties of the sequence spaces S^ν, J. Math. Anal. Appl. 1 (2006) 364–387.
[20] B. Mandelbrot, J. van Ness, Fractional Brownian motions, fractional noises and applications, SIAM Rev. 10 (1968) 422–437.

Please cite this article in press as: C. Esser et al., A multifractal formalism for non-concave and non-increasing spectra: The leaders profile method, Appl. Comput. Harmon. Anal. (2016), http://dx.doi.org/10.1016/j.acha.2015.12.006

[21] J.-P. Kahane, Some Random Series of Functions, Cambridge University Press, 1993.
[22] F. Comte, E. Renault, Long memory in continuous-time stochastic volatility models, Math. Finance 8 (1998) 291–323.
[23] B. Audit, C. Thermes, C. Vaillant, Y. d'Aubenton Carafa, J.-F. Muzy, A. Arneodo, Long-range correlations in genomic DNA: a signature of the nucleosomal structure, Phys. Rev. Lett. 86 (2001) 2471.
[24] S. Nicolay, M. Touchon, B. Audit, Y. d'Aubenton Carafa, C. Thermes, A. Arneodo, et al., Bifractality of human DNA strand-asymmetry profiles results from transcription, Phys. Rev. E 75 (2007) 032902.
[25] A. Wood, G. Chan, Simulation of stationary Gaussian processes in $[0,1]^d$, J. Comput. Graph. Statist. 3 (1994) 409–432.
[26] J.-F. Muzy, Analyse de distributions fractales à partir de leur transformée en ondelettes, Ann. Phys. Fr. 20 (1995) 63–231.
[27] S. Raible, Lévy processes in finance: theory, numerics, and empirical facts, Ph.D. thesis, 2000.
[28] S. Jaffard, The multifractal nature of Lévy processes, Probab. Theory Related Fields 114 (1999) 207–227.
[29] R.N. Mantegna, Fast, accurate algorithm for numerical simulation of Lévy stable stochastic processes, Phys. Rev. E 49 (1994) 4677–4683.
[30] J. Barral, S. Seuret, From multifractal measures to multifractal wavelet series, J. Fourier Anal. Appl. 11 (2005) 589–614.
[31] B. Testud, Étude d'une classe de mesures autosimilaires: calculs de dimensions et analyse multifractale, Ph.D. thesis, 2004.
[32] S. Seuret, Detecting and creating oscillations using multifractal, Math. Nachr. 279 (11) (2006) 1195–1211.

Please cite this article in press as: C. Esser et al., A multifractal formalism for non-concave and non-increasing spectra: The leaders profile method, Appl. Comput. Harmon. Anal. (2016), http://dx.doi.org/10.1016/j.acha.2015.12.006